RSC Advances

PAPER

View Article Online
View Journal | View Issue

Cite this: *RSC Adv.*, 2020, **10**, 32357

Yttrium(III) coordination polymer micro/nanospheres with single ligand and dual ligands†

Yanhua Ji,[a] Qifeng Guo,[b] Qingquan Yang,[b] Yong Gao,[b] Xiaojun Yan,[b] Hongning Liu[b] and Zhijun Zeng *[ab]

Received 17th June 2020
Accepted 12th August 2020

DOI: 10.1039/d0ra05325b

rsc.li/rsc-advances

In this work, yttrium(III) coordination polymer (Y-CP) ball-flower-shaped microparticles with diameters ranging from 5 μm to 10 μm were synthesized using vanillin and asparagine as ligands under solvothermal conditions at 150 °C for 24 h. Then, we investigated the reaction influencing factors such as the concentration of reactants (involving vanillin, asparagine, and rare earth), reaction temperature, and reaction time. Both uniform and sphere-like nanoparticles with an average size of ~50 nm were obtained using vanillin as a ligand at 120 °C for 12 h. Furthermore, the products were characterized and the results of cytotoxicity research demonstrated that the nanoparticles had low cytotoxicity and the coordination polymer nanospheres were perfectly biocompatible.

1. Introduction

In the last few decades, there has been considerable interest in rare-earth-based coordination polymers (RE-CP). Inorganic–organic hybrid materials are very important because they have many potential applications in a broad range of fields such as chemical sensing, lighting and display[1–7] bioapplications,[8,9] and thermometric probes.[1,10] Lanthanide materials are very useful in many applications.[11,12] For example, YVO_4 nanoparticles are known to be useful probes for biological applications.[13]

In this study, yttrium has been selected as it is one of the most abundant rare earth elements. Because of its unique physical properties, it has been extensively studied in the fields of laser materials,[14] new magnetic materials,[15] nuclear fuel cladding materials,[16] and other materials. Moreover, due to the anti-tumor activity of rare-earth complexes, yttrium has a significant influence in the medical field.[17,18]

Ce-CP flowerlike micro/nanostructures have been prepared and this structure shows optical and magnetic properties.[19] This type of flower-like micro/nanostructures have excellent physical and chemical properties because of their unique structures and large specific surface area.[20] With the development of biomaterial applications, lanthanide complexes have attracted considerable attention. If ligands own certain functional groups such as maleimide, amino, and carboxyl groups, they could show successful bioapplications.[21–23,37] However, as a biomaterial, controlling the morphology, structure and size of the micro/nanoparticles is important.[5,21,24]

Ortho-vanillin is a popular ligand in coordination chemistry because it is a Schiff base that generates rich multifarious coordination polymers.[1] Especially, complexes were synthesized from dual ligands, *i.e.*, vanillin and asparagine. The complexes have various interesting properties such as cytotoxicity and luminescence. Furthermore, the morphology and structure of the lanthanide coordination polymers are affected by several factors, such as the molar ratio of ligand (including vanillin, asparagine) and rare earth,[25,26] reaction temperature,[25,27–30] pH,[25,27,28] and reaction time.

In this study, we synthesized the yttrium(III) coordination polymer (Y-CP) with different morphologies with a single ligand and dual ligands using a solvothermal method. The solvothermal method is developed from the hydrothermal method, and the reaction process was simple and easy to control, as well as had a wide range of applications in synthetic chemistry.[31–33] To date, few studies have reported this type of a synthetic method; however, there has been no successful report related to the preparation of 3D micro ball-flower-like coordination polymer from yttrium(III). Therefore, the ball-flower-like samples will be discussed herein. Uniform and sphere-like nanoparticles with an average size of ~50 nm were then obtained and investigated in this study.

2. Experimental

In this work, Y-CP micro/nanospheres were prepared. In a typical procedure (Scheme 1), 0.3 mmol of vanillin and 0.3 mmol of asparagine were placed in a 25 ml teflon-lined stainless steel autoclave. Then, the chemicals were dissolved in 10 ml of distilled water under magnetic stirring. Then, 0.2 mmol Y^{3+} was added to the above solution, and the

[a]University of Jiangxi TCM, Nanchang 330006, China. E-mail: zhijunzeng@aliyun.com
[b]Research Center for Differention and Development of TCM Basic Theory, Jiangxi Province Key Laboratory of TCM Etiopathogenisis, University of Jiangxi TCM, Nanchang 330006, China

† Electronic supplementary information (ESI) available. See DOI: 10.1039/d0ra05325b

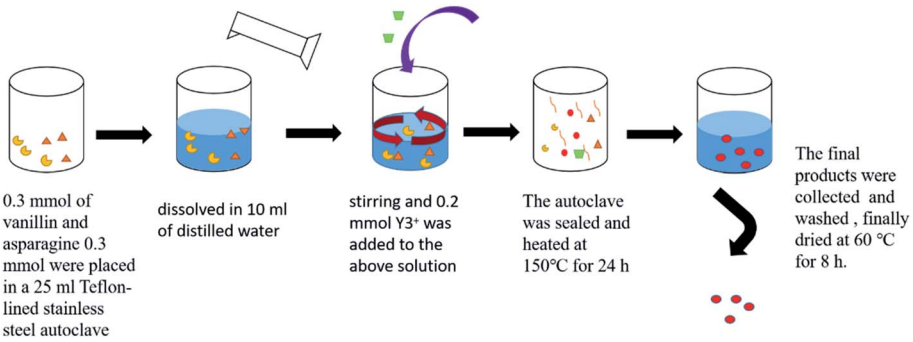

Scheme 1 Flow diagram for the synthesis of the coordination polymer.

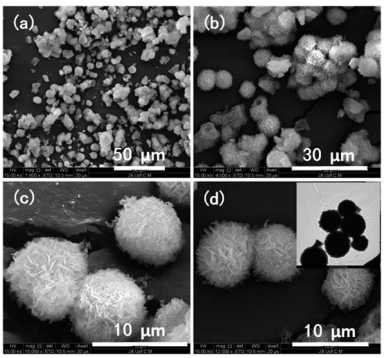

Fig. 1 Images of SEM (a–d) and TEM (d) of the product obtained sample 1.

autoclave was sealed and heated at 150 °C for 24 h. The final products were collected by centrifugation and washed several times with ethanol and distilled water. Finally, the precipitate was dried at 60 °C for 8 h.

The MTT assay was used to detect the viability of HeLa cells exposed to nanospheres. In brief, $\sim 10^4$ cells were seeded per well of the 96-well plate; after overnight incubation, the samples in phosphate-buffered saline were added to each cell with their concentrations ranging from 20 to 100 μg ml^{-1} at 37 °C. After incubation for 48 h, MTT was added to each well, and incubation was continued for 4 h. All media was removed and dimethyl sulfoxide was added to each well, and then absorbance was measured using a microplate reader.

3. Results and discussion

We characterized the samples to obtain the required data. Firstly, FT-IR spectroscopy was performed to determine whether there was coordination polymer formation. Secondly, SEM was used to observe its microstructure and size to determine whether it could be used in cell experiments and mass production. Then, we used XRD, EDS, TG, and DTA to infer the chemical formula of the complex. Finally, we carried out cytotoxicity experiments to explore whether it could be used as a biomaterial. Therefore, the results could be useful for future work.

The SEM technique was used to characterize the morphology, structure, and size of products. The SEM image (Fig. 1a) shows a representative morphology; these microspheres are composed of uniform micro-ball-flower-like and can be prepared on a large scale. The enlarged SEM image (Fig. 1b) clearly reveals that the as-synthesized product comprises a micro-ball-flower with a diameter varying from 5 to 10 μm. The other enlarged SEM and TEM images (Fig. 1c and d) of the product confirms the SEM results (Fig. 1b).

XRD pattern of the sample 1 product (other samples XRD patterns can be seen in ESI†) is shown in Fig. 2a. It obviously shows that sample 1 is amorphous. The FT-IR spectrum of Y-CP is shown in Fig. 2b. It turns out that the absorption peak at 3500 cm^{-1} could be assigned to –OH because its oxygen atoms coordinate with rare-earth ions. Moreover, it causes the absorption peak to shift to blue, thus breaking the hydrogen bonds in the molecule. The FT-IR results prove the formation of the

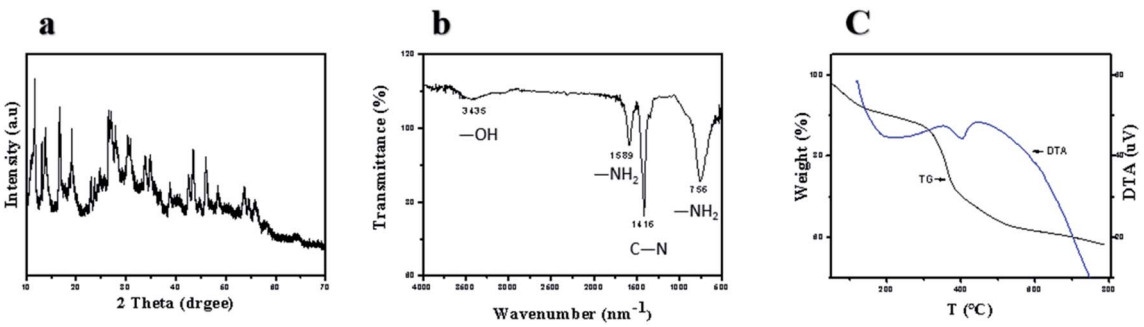

Fig. 2 (a) XRD pattern, (b) IR spectrum and (c) TG-DTA curves of sample 1.

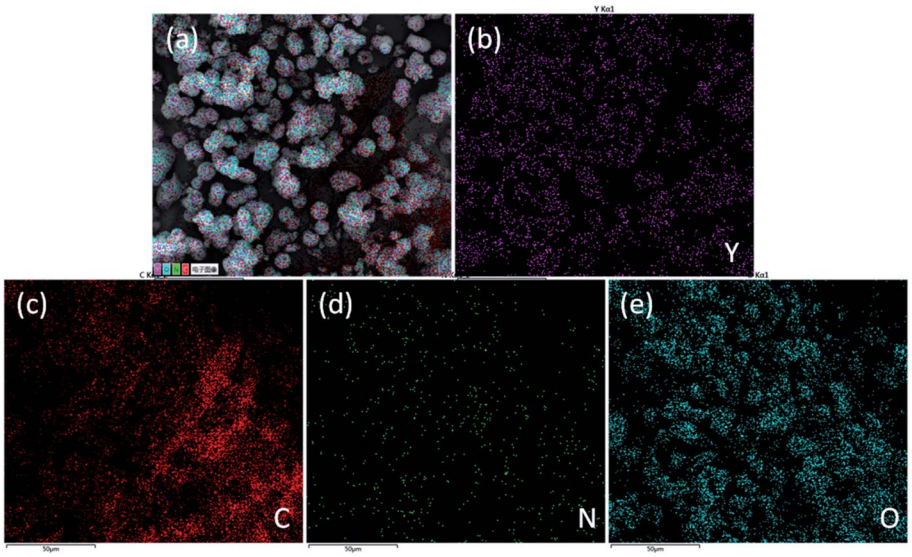

Fig. 3 Distribution diagrams of integrated elements (a) and elements of yttrium (b), carbon (c), oxygen (d), nitrogen (e).

coordination polymer. Both TG and DTA (Fig. 2c) were measured under atmospheric conditions. TG analysis shows that the first mass loss in the range of 50 to 300 °C is 13.0%, indicating the loss of the physically absorbed water molecules and dimethylformamide molecules. An apparent weight loss between 300 and 530 °C is ascribed to the decomposition of asparagine and vanillin frameworks. At this stage, $Y(OH)_3$ is produced, which reacts with CO_2 to produce $Y_2O_2CO_3$. Note that $Y_2O_2CO_3$ decomposes between 530 and 800 °C. Both TG and DTA curves were similar to the decomposition of $La(OC_2H_4OH)_3$.[3,21]

The element distribution in the sample was obtained using EDS (Fig. 3). The yttrium distribution is shown in Fig. 3b. Fig. 4c shows the distribution of carbon, and the distribution of oxygen and nitrogen are shown in Fig. 4d and 5e, respectively. The distribution of nitrogen is observed to a lesser extent. Based on the abovementioned results, the formula of the product can be proposed as $C_8H_8O_3 \cdot C_4H_8N_2O_3 \cdot Y$.

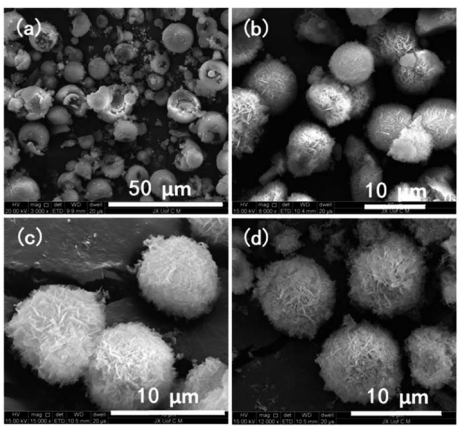

Fig. 4 SEM images show that the ratio of ligands to rare earth were 3 : 3 : 2 (a, sample 2), 3 : 3 : 4 (b, sample 3), 3 : 3 : 5 (c, sample 1), and 3 : 3 : 6 (d, sample 4).

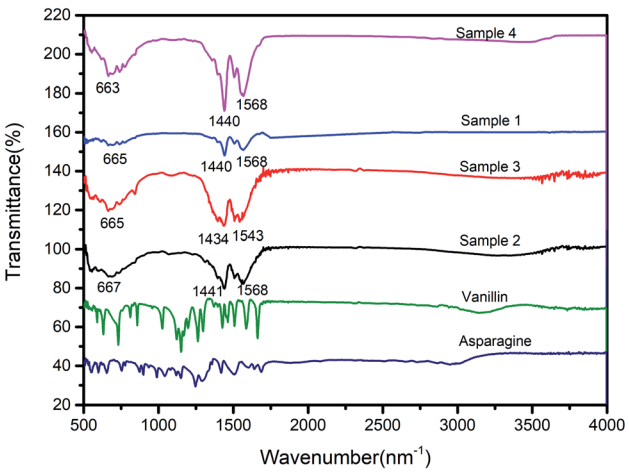

Fig. 5 IR spectra of sample 2, sample 3, sample 1, sample 4, vanillin, and asparagine.

A range of controlled experiments were performed. The experiments were carried out at different levels of Y^{3+} in the reaction. Therefore, additional SEM images (Fig. 4) were

Table 1 Molar ratios of the corresponding ligands to rare-earth for samples 1–5

	Ligands		
Sample	Vanillin	Asparagine	Y
1	3	3	5
2	3	3	2
3	3	3	4
4	3	3	6
5	3	—[a]	3

[a] "—" represent that the ligand is not used in the sample.

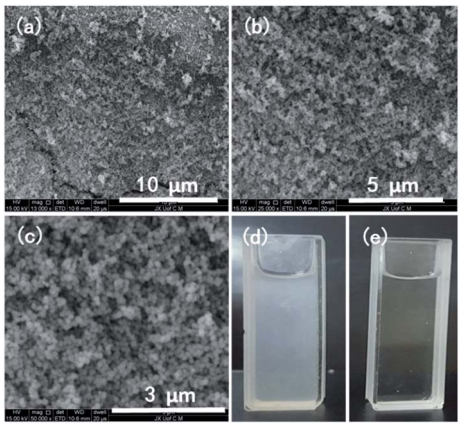

Fig. 6 (a–c) SEM images of the product (sample 2); (d) sample 2 nanospheres with a concentration of 150 μg ml^{-1} after 6 days and (e) the above solution obtained after centrifuging (d) at 10 000 rpm.

captured, showing the morphology and structural features. The molar ratio of ligands and rare earths were 3 : 3 : 2 (Fig. 4a), 3 : 3 : 4 (Fig. 4b), 3 : 3 : 5 (Fig. 4c), and 3 : 3 : 6 (Fig. 4d). The molar ratios of the corresponding ligands to rare-earth in samples 1–5 are summarized in Table 1. A ball-flower-like morphology was obtained when the ratio was 3 : 3 : 4 (Fig. 4b). However, the ball-flower-like structure was not formed when the molar ratio was 3 : 3 : 2 (Fig. 4a). The SEM image shows that the product morphology is ball-like; however, the balls were split and broken. When the molar ratio of Y^{3+} was increased to 3 : 3 : 6 (Fig. 4d), the morphology of the sample did not change. Furthermore, the images show the ball-flower-like morphology with good dispersity.

FTIR spectra of samples with different contents of Y^{3+} in Y-CP are shown in Fig. 5. There is no discernible difference in the FT-IR spectra. The absorption peak at 3500 cm^{-1} is assigned to –OH because its oxygen atoms coordinate with rare-earth ions. The FTIR results confirm the formation of the coordination polymer.

We also synthesized materials under similar reaction conditions but without the addition of asparagine. There was a remarkable influence on the morphology of the products. In Fig. 6, the sample 5 with nanosphere shape with a size of ~20–50 nm was formed. Moreover, this product showed good dispersibility when sample 5 was dispersed in water. After 7 days, the dispersed solution was still very stable (Fig. 5d and e).

TG and DTA (see Fig. 7c) were measured under atmospheric conditions. TG analysis shows that the first mass loss was in the range of 50–300 °C, indicating the loss of the physically absorbed water molecules and dimethylformamide molecules. The weight loss between 300 and 530 °C is ascribed to an apparent decomposition of the vanillin frameworks. In this process, $Y(OH)_3$ was produced, which reacts with CO_2 to produce

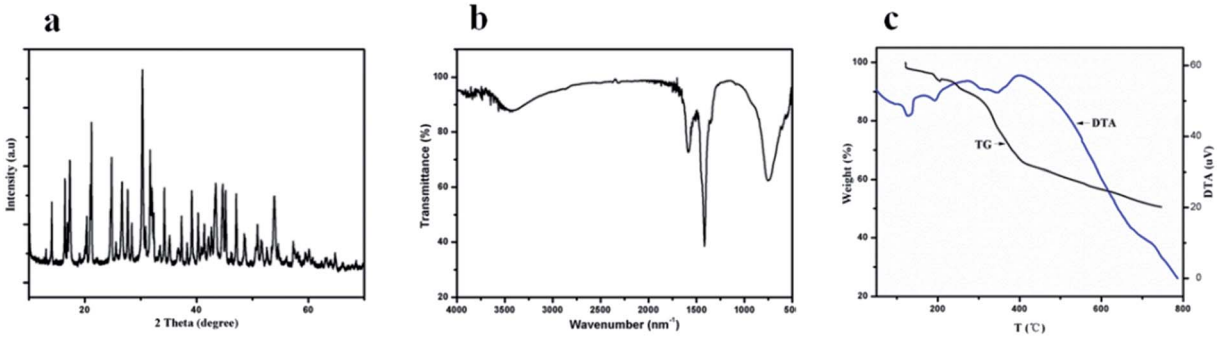

Fig. 7 (a) XRD pattern, (b) IR spectrum and (c) TG-DTA curves of sample 2.

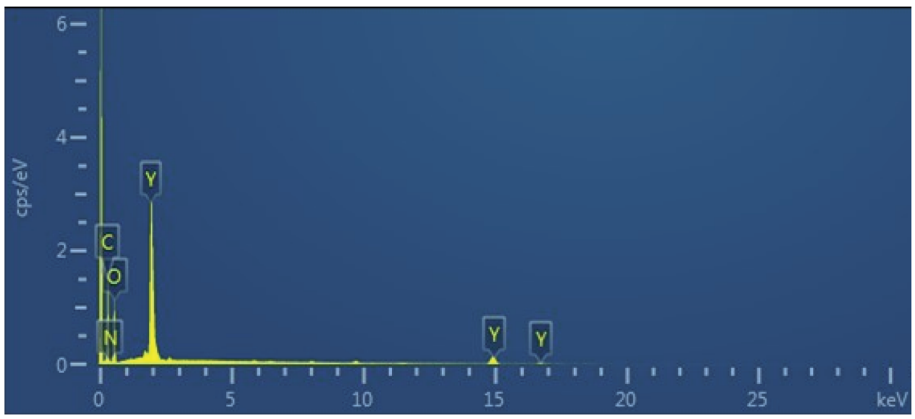

Fig. 8 Elemental distribution of sample 5.

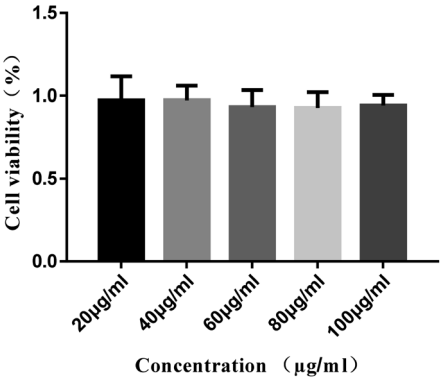

Fig. 9 Viability of cells exposed to different concentrations of the coordination polymers nanospheres (sample 5).

$Y_2O_2CO_3$. The formed $Y_2O_2CO_3$ was then decomposed between 530 and 800 °C. The TG and DTA curves were similar to the decomposition pattern of $La(OC_2H_4OH)_3$.[21,34]

The element distribution of the sample was obtained by EDS (Fig. 8). The image shows that the sample contained yttrium, carbon, and oxygen.

Cytotoxicity experiment results are shown in Fig. 9. The living cells are ~98% at the concentration of 100 μg ml^{-1}, and the morphology of sample 5 is nanosphere with a size of ~20–50 nm. The results indicated that sample 5 has good biocompatibility[35] and low cytotoxicity. Moreover, the cytotoxicity of sample 5 was lower than that of inorganic materials.[19,36] Therefore, it can use as a biomaterial.

4. Conclusions

In summary, we successfully synthesized yttrium(III) coordination polymer micro/nanospheres with a single ligand and dual ligands for the first time. It can be concluded from the results of the study that in the dual-ligand approach, the microstructure of the product gradually tends to be a complete ball-flower-like with the increase of Y^{3+} content at constant ligands concentrations. That is to say, the content of rare earth determines the microstructure of the product in this case. It is worth mentioning that when a single ligand is used, the products obtained are nanoscale rather than micro scale, showing better good biocompatibility, low cytotoxicity and good dispersibility in water. Because of the low cytotoxicity, extensive bioapplications can be identified.

Conflicts of interest

There is no conflict of interest.

Acknowledgements

This research work was supported by National Natural Science Foundation of China (81760787), Scientific Foundation of the Education Department of Jiangxi Province (GJJ190643), Traditional Chinese medicine Scientific Research Subject of Jiangxi Province (2019A111), Health and Family Planning Commission of Jiangxi province (20195651 and 20203772), Research Center of Natural Resources of Chinese Medicinal Materials and Ethnic Medicine (JXXT2018002) and the specialized research fund for the first-class discipline of Chinese herb from Jiangxi province (JXSYLXK-ZHYAO111).

References

1 M. Andruh, The exceptionally rich coordination chemistry generated by Schiff-base ligands derived from *o*-vanillin, *Dalton Trans.*, 2015, **44**(38), 16633–16653.
2 B. B. C. Holanda, R. B. Guerra, A. O. Legendre, D. F. Almeida, T. F. C. Fragasilva, C. F. Ângela, J. Venturini and G. Bannach, Thermal, spectroscopic and biological studies on solid ibuprofen complexes of heavy trivalent lanthanides and yttrium, *Thermochim. Acta*, 2017, **647**, 47–54.
3 H. Zhao, X. X. Sun, H. M. Hu, R. An, M. L. Yang and G. Xue, Syntheses, Structures and Luminescent Properties of Lanthanide Coordination Polymers Assembled from Imidazophenanthroline Derivative and Oxalate Ligands, *J. Solid State Chem.*, 2017, **245**, 67–73.
4 B. Golesorkhi, H. Nozary, A. Furstenberg and C. Piguet, Erbium complexes as pioneers for implementing linear light-upconversion in molecules, *Mater. Horiz.*, 2020, **7**(5), 1279–1296.
5 M. Manimohan, S. Pugalmani, K. Ravichandran and M. A. Sithique, Synthesis and characterisation of novel Cu(II)-anchored biopolymer complexes as reusable materials for the photocatalytic degradation of methylene blue, *RSC Adv.*, 2020, **10**(31), 18259–18279.
6 Y. Hasegawa and Y. Kitagawa, Thermo-sensitive luminescence of lanthanide complexes, clusters, coordination polymers and metal–organic frameworks with organic photosensitizers, *J. Mater. Chem. C*, 2019, **7**(25), 7494–7511.
7 Y. B. Fu, X. Wane and M. Y. Peng, Tunable photoluminescence from $YTaO_4$:Bi^{3+} for ultraviolet converted pc-WLED with high chromatic stability, *J. Mater. Chem. C*, 2020, **8**(18), 6079–6085.
8 Z. Wang, J. G. Li, Z. Qi, B. N. Kim and X. Sun, Dicarboxylate mediated efficient morphology/phase tailoring of YPO_4:Ln^{3+} crystals and investigation of down-/up-conversion luminescence, *CrystEngComm*, 2017, **19**(35), 5230–5243.
9 B. Wu, L. J. Zhao, Y. Wang, H. T. Dong and H. Yu, Er^{3+}/Yb^{3+} co-doped nanocrystals modified with 6-aminocaproic acid for temperature sensing in biomedicine, *RSC Adv.*, 2019, **9**(72), 42228–42235.
10 Z. U. Nisa, L. Tashi, C. Sen, N. A. Ashashi, S. C. Sahoo and H. N. Sheikh, Synthesis of eight isostructural 2D lanthanide coordination polymers assembled by rigid furan-2,5-dicarboxylic acid and flexible adipic acid as linkers and exploration of luminescent Eu/Tb polymers as efficient and sensitive sensors for nitroaromatic compounds, *New J. Chem.*, 2020, **44**(19), 8125–8137.
11 T. D. S. Heikham Farida Devi, Morphology control synthesis and photoluminescence of yttrium orthophosphate microstructures, *Mater. Lett.*, 2018, **231**, 8–10.

12 Sb Xia, F. S. Li, X. Shen, X. Li, F. X. Cheng, C. K. Sun, H. Guo and J. J. Liu, A lanthanide-based coordination polymer as lithium ion battery anode with high cyclic stability, *Mater. Lett.*, 2019, **238**, 171–174.

13 H. Wang, O. Odawara and H. Wada, Morphology and optical properties of YVO_4:Eu^{3+} nanoparticles fabricated by laser ablation in ethanol, *Appl. Surf. Sci.*, 2017, **425**, 689–695.

14 A. Sposito, S. A. Gregory and R. W. Eason, Selective growth of yttrium iron garnet and yttrium ferrite by combinatorial pulsed-laser ablation of common precursors, *J. Mater. Sci.*, 2014, **49**(15), 5462–5467.

15 N. V. Vorob'eva and V. B. Mityukhlyaev, Features of photoinduced magnetism in some yttrium-iron-garnet single crystals, *Semiconductors*, 2016, **50**(4), 449–452.

16 V. Firouzdor, J. Brechtl, L. Wilson, B. Semerau, K. Sridharan and T. R. Allen, Development of Yttrium Stabilized Zirconia (YSZ) diffusion barrier coatings for mitigation of Fuel-Cladding Chemical Interactions, *J. Nucl. Mater.*, 2013, **438**(1–3), 268–277.

17 A. Caporale, G. Palma, A. Mariconda, *et al.*, Synthesis and Antitumor Activity of New Group 3 Metallocene Complexes, *Molecules*, 2017, **22**(4), 1–13.

18 W. Y. Zhong, Z. X. Hu, S. F. Chen, S. Y. Ji, Y. P. Zhou and Ml Li, Synthesis, structure characterization and anti-tumor activity of lanthanide complex $Ln(Phen)_2(5\text{-}Fu)_3(NO_3)(NO_3)_2$, *Acta Pharm. Sin. B*, 2005, **40**(11), 997–1000.

19 S. Zhong, M. Wang, W. Lei, L. Yuan, H. M. Noh and J. H. Jeong, Preparation of 3D cerium-based coordination polymer microstructures and their conversion to ceria, *CrystEngComm*, 2014, **16**(2), 231–236.

20 S. Wei, R. Zhou and G. Wang, Enhanced Electrochemical Performance of Self-Assembled Nanoflowers of MoS_2 Nanosheets as Supercapacitor Electrode Materials, *ACS Omega*, 2019, **4**(14), 15780–15788.

21 S. Zhong, Y. Ji, Q. Xie, W. Lei, L. Yuan and J. H. Jeong, Coordination polymer nanospheres: preparation, upconversion properties and cytotoxicity study, *Mater. Lett.*, 2013, **102**(13), 19–21.

22 C. Xiao, H. L. Xu and S. L. Zhong, Au@Eu-based coordination polymers core–shell nanoparticles: photoluminescence and photothermal properties, *Mater. Lett.*, 2018, **216**, 106–109.

23 F. Wu, D. F. He, L. Chen, F. Q. Liu, H. L. Huang, J. S. Dai, S. Y. Zhang and J. S. You, Antibacterial coordination polymer hydrogels composed of silver(I)-PEGylated bisimidazolylbenzyl alcohol, *RSC Adv.*, 2018, **8**(37), 20829–20835.

24 M. Jost, R. M. Richter, M. Balmer, B. Peters, F. Dankert and C. von Hanisch, Coordination polymers of alkali metal cyclosiloxazanides with one- and two-dimensional structures, *Dalton Trans.*, 2020, **49**(18), 5787–5790.

25 Z. He, Y. Yang, J. W. Liu and S. H. Yu, Emerging tellurium nanostructures: controllable synthesis and their applications, *Chem. Soc. Rev.*, 2017, **46**(10), 2732–2753.

26 L. He, X. Li, Y. Yang, Q. J. Zheng, N. Jiang, C. G. Xu, Y. F. Liu and D. M. Lin, Morphology-controlled synthesis, growth mechanism and fluorescence of YF_3:Eu^{3+},Bi^{3+}, *Mater. Res. Bull.*, 2017, **95**, 483–490.

27 L. Hernandez-Adame, N. Cortez-Espinosa, D. P. Portales-Perez, C. Castillo, W. Zhao, Z. N. Juarez, L. R. Hernandez, H. Bach and G. Palestino, Toxicity evaluation of high-fluorescent rare-earth metal nanoparticles for bioimaging applications, *J. Biomed. Mater. Res., Part B*, 2017, **105**(3), 605–615.

28 H. X. Guan, C. Xu, Y. Sheng, Y. H. Song, K. Y. Zheng, Z. Shi and H. F. Zou, Controlling the Morphology and Size of GdF_3:RE^{3+} (RE = Dy, Tb, and Sm) by pH Value: Growth Mechanism, Energy Transfer, and Luminescent Properties, *J. Phys. Chem. C*, 2017, **121**(12), 6884–6897.

29 X. Zou, L. He, D. Tan, F. Lei, N. Jiang, Q. Zheng, D. Lin, C. Xu and Y. Liu, Anneal-induced transformation of phase structure, morphology and luminescence of $GdPO_4$:Sm(3+) nanomaterials synthesized by a hydrothermal method, *Dalton Trans.*, 2017, **46**(9), 2948–2956.

30 S. Wang, Y. Li, Y. Zhang, S. Wang and Z. Tan, Synthesis, characterization, thermal, electrical and magnetic properties of polyaniline composites with rare earth gadolinium coordination complex, *Polym. Adv. Technol.*, 2016, **28**(3), 411–420.

31 W. X. Chen, H. P. Chen, H. T. Zhu, Q. Q. Gao, J. Luo, Y. Wang, S. Zhang, K. Zhang, C. M. Wang, Y. J. Xiong, Y. F. Wu, X. S. Zheng, W. S. Chu, L. Song and Z. Y. Wu, Solvothermal Synthesis of Ternary Cu_2MoS_4 Nanosheets: Structural Characterization at the Atomic Level, *Small*, 2014, **10**(22), 4637–4644.

32 L. Q. Kong, D. P. Zhang, D. C. Li and J. M. Dou, Solvothermal Synthesis and Characterization of Two New Nickel Nido-Carborane Diphosphine Complexes, *J. Cluster Sci.*, 2011, **22**(1), 97–105.

33 M. Mastalir, C. Schweinzer, M. Weil, E. Pittenauer, G. Allmaier and K. Kirchner, A chromium tricarbonyl complex featuring the 4,6-bis(diphenylphosphinomethyl) dibenzothiophene (PSPPh) ligand, *Monatsh. Chem.*, 2016, **147**(7), 1183–1187.

34 S. Zhong, B. Deng, A. Xu and S. Wang, Preparation and Characterization of 3D Flower-like La_2O_3 Nanostructures, *Curr. Nanosci.*, 2011, **7**(3), 407–411.

35 Z. J. Zeng, Y. H. Ji, X. Huang, Y. N. Jiang, Z. M. Ou, W. P. Xiong, B. T. Li, Q. Y. Zhang, P. Nie, G. L. Xu and H. N. Liu, Integrating the Metpa and Ipa To Verify the Biological Function of the Potential Biomarkers from Plasma Metabonomics in Diabetic Rats, *Acta Med. Mediterr.*, 2019, **35**(3), 1627–1631.

36 J. Zhou, Z. Liu and F. Li, Upconversion nanophosphors for small-animal imaging, *Chem. Soc. Rev.*, 2012, **41**(3), 1323–1349.

37 Q. Zeng, Y. Liu, Y. Song, B. Feng, P. Xu, B. Shan, Z. Liao, K. Liu, Y. Zhong, L. Chen and D. Su, A UHPLC-MS/MS method coupled with simple and efficient alkaline hydrolysis for free and total determination of conjugate nanomedicine: Pharmacokinetic and biodistribution study of poly (l-glutamic acid)-graft-methoxy poly (ethylene glycol)/combretastatin A4, *J. Pharm. Biomed. Anal.*, 2019, **169**, 215–224.

